

## Supporting information

### Epoxides hydrolysis and alcoholysis reactions over crystalline Mo–V–O oxide

Xiaochen Zhang <sup>a</sup>, Min Wang <sup>a</sup>, Chaofeng Zhang <sup>a,b</sup>, Jianmin Lu <sup>a</sup>, Yehong Wang <sup>a</sup>, Feng Wang <sup>a\*</sup>

<sup>a</sup> State Key Laboratory of Catalysis, Dalian National Laboratory for Clean Energy,  
Dalian Institute of Chemical Physics, Chinese Academy of Sciences, Dalian 116023, Liaoning, China

<sup>b</sup> Graduate University of Chinese Academy of Sciences, Beijing 100049, China

\*Corresponding author.

Tel: +86-411-84379762; Fax: +86-411-84379762; E-mail: wangfeng@dicp.ac.cn

## Materials

All chemicals were of analytical grade and used as purchased without further purification. Most materials were purchased from Tianjin Kermel Chemical Reagent Co. Ltd.  $\text{VOSO}_4 \cdot n\text{H}_2\text{O}$  (64.83 wt%) was obtained from Shanghai Huating Chemicals Factory Co. Ltd..

## Mo-V-O materials synthesis

The Mo-V-O materials were synthesized by hydrothermal method. An amount of aqueous solution of  $\text{VOSO}_4 \cdot n\text{H}_2\text{O}$  was dropped into the aqueous solution of  $(\text{NH}_4)_6\text{Mo}_7\text{O}_{24}$  with stirring for ten minutes at ambient temperature. The mixture was transferred into an autoclave with a Teflon inner tube and Teflon thin sheet, and bubbled with  $\text{N}_2$  to remove the oxygen. The pH for preparation of the orthorhombic material is about 3.2. Then hydrothermal synthesis is continued for 48 h at 175 °C. The obtained gray solid was separated by filtration, washing and drying. The obtained solid (1 g) was purified with 50 mL oxalic acid of 0.4 mol  $\text{L}^{-1}$  and washed to neutral and dried. The preparation of trigonal material followed the same procedures as the above, except that the pH was adjusted to 2.2 using  $\text{H}_2\text{SO}_4$  (9 vol %). The tetragonal material was prepared by heat-treatment of the orthorhombic material in air for 2 h at 400 °C and then in nitrogen for 2 h at 575 °C with a heating rate of 10 °C  $\text{min}^{-1}$ .

## Characterization

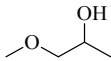
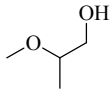
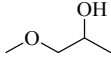
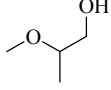
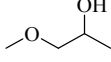
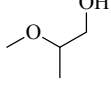
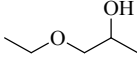
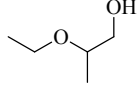
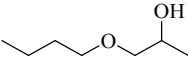
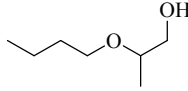
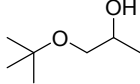
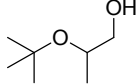
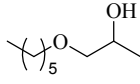
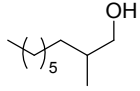
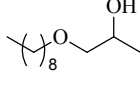
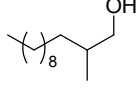
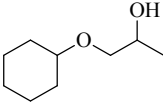
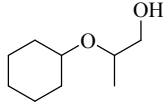
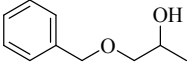
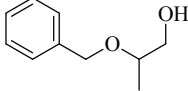
The morphology of the materials was characterized by scanning electron microscopy on JSM-7800F (Japan). The powder XRD patterns were measured on X'pert Pro-1 X-ray diffractometer (Netherlands) with Cu Ka (tube voltage: 40 kV, tube current: 30 mA, Scan rate 10 °C  $\text{min}^{-1}$ ). The infrared (FT-IR) spectra were measured as KBr disks on a Bruker Tensor 27 FT-IR spectrometer (Germany) with 16 scan at a resolution of 4  $\text{cm}^{-1}$ . The  $^1\text{H}$  NMR and  $^{13}\text{C}$  NMR spectra of products were characterized with liquid nuclear magnetic resonance spectrometer (AVANCE III HD 700MHz).

The acidity was measured by  $\text{NH}_3$ -TPD with ThermoStar<sup>TM</sup> (Germany), gas flow 50 mL  $\text{min}^{-1}$ . Before measurements, the samples were treated at the  $\text{N}_2$  flow at 100 °C to remove the adsorbed surfaced species. Then  $\text{NH}_3$  was introduced and pass through the sample. The adsorption of  $\text{NH}_3$  was maintained until the adsorption peak intensity of  $\text{NH}_3$  was not increased. Finally, the  $\text{NH}_3$  adsorbed by the sample was desorbed with temperature rising (10 °C  $\text{min}^{-1}$ ) till the desorption line equilibrium.

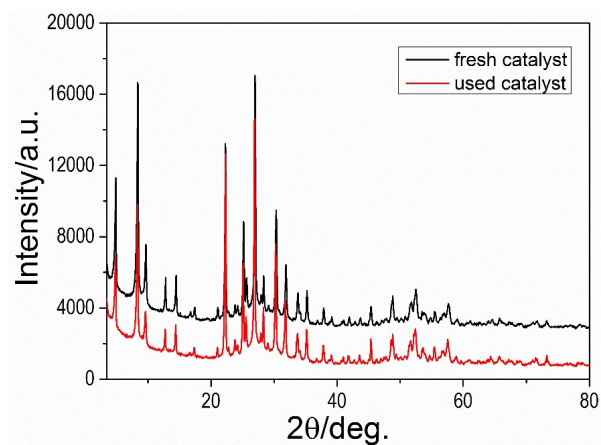
## Catalytic test

Catalytic reactions were carried out in a 15-mL pressure bottle under stirring. The catalyst (0.01 g) was added to the distilled water (1 mL) containing 3 mmol of epoxide. The reaction was continued at a desired temperature. After reaction, the residue was extracted and filtered out using membrane filter. The filtrate was analyzed in GC-MS and GC (7890). The conversion of epoxide and yield of ring-opening products were quantified using internal standard (1,3,5-trimethyl-benzen).

**Table S1** Alcoholysis of propylene oxide with different alcohols in different conditions

Entry	Substrate	Product		Conv./%	Sel./%
1 <sup>b</sup>	MeOH			79	44/54
2 <sup>c</sup>	MeOH			90	47/53
3 <sup>d</sup>	MeOH			>99	39/54
4	EtOH			79	39/53
5	n-BuOH			64	32/61
6	t-BuOH			24	31/34
7	n-pentanol			56	31/61
8	n-Octanol			50	31/68
9	cyclohexanol			39	24/42
10	benzyl alcohol			36	35/52

Reaction conditions: 3 mmol propylene oxide, 1 mL alcohol, 0.01 g trigonal Mo-V-O, 100 °C, 8 h.

**Fig. S1** XRD patterns of fresh and used crystalline trigonal Mo-V-O.

The catalysts after reaction show similar structure with the fresh catalyst measured by the XRD.

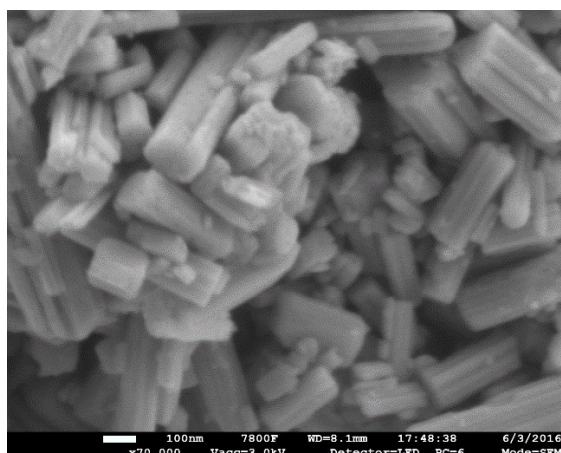


Fig. S2 The SEM images of used trigonal Mo-V-O (milling time-10 min). The catalyst material after the reaction still keep the morphology of rod crystal, and there is no obvious change in the average particle size.

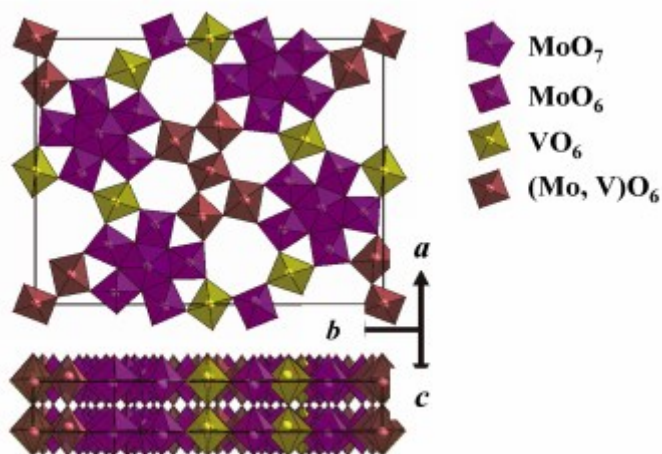


Fig. S3 The scheme with the structure of the trigonal Mo-V-O. The scheme with the structure of the trigonal Mo-V-O derived from the literature: Ueda, J Jpn Petrol Inst, 2013, 56, (3), 122-132.

In the hydrolysis and alcoholysis catalysis, we identified the final products by matching the GC-MS spectrum of the products with the standard spectrum. Some GC-MS spectrum of the products selected are showed as follows (Fig. S4- Fig. S17):

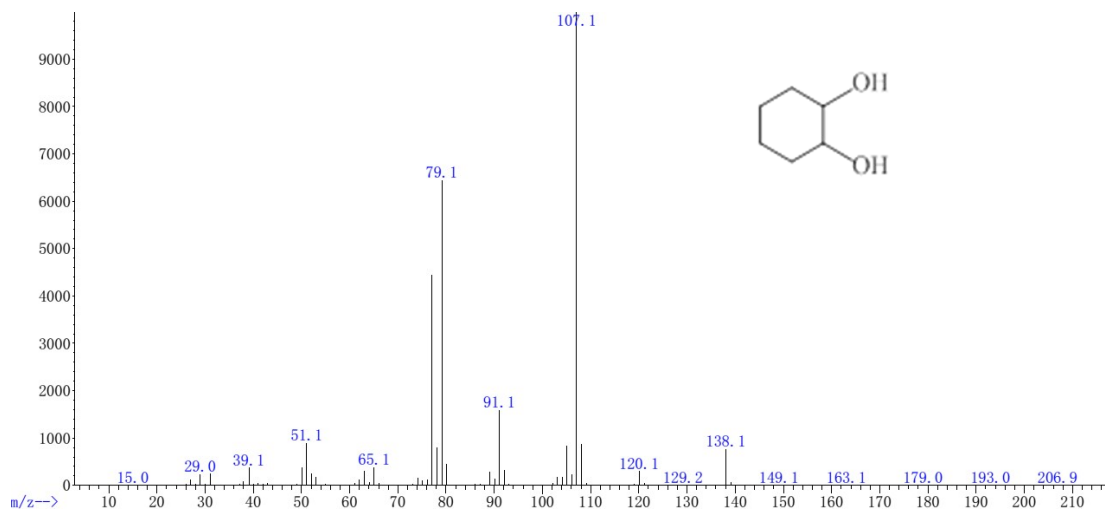


Fig. S4

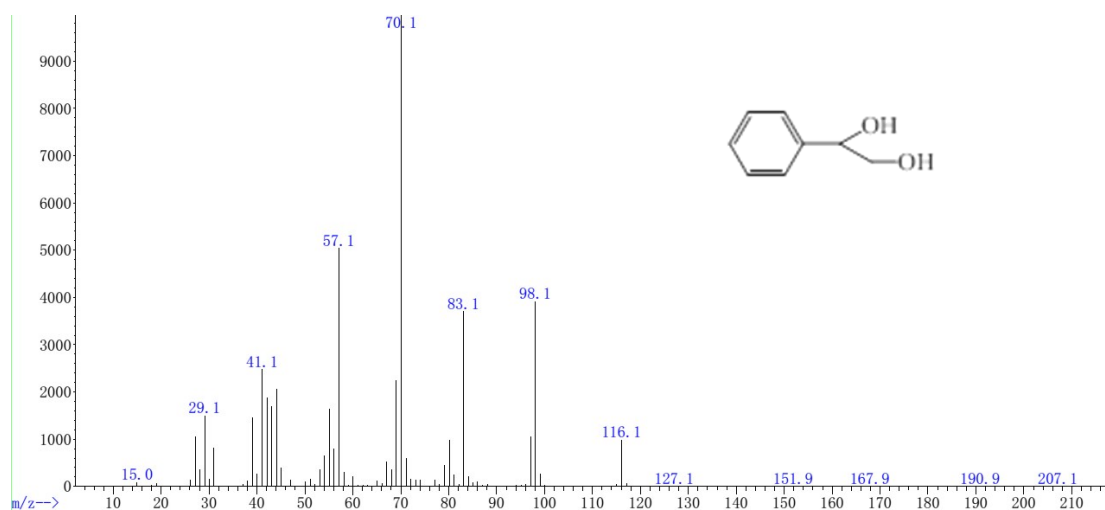


Fig. S5

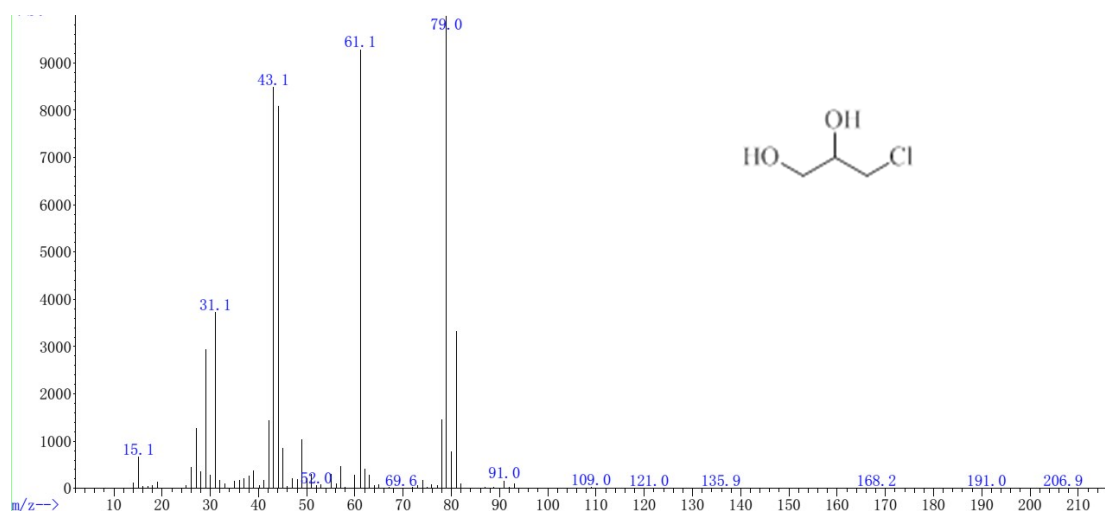


Fig. S6

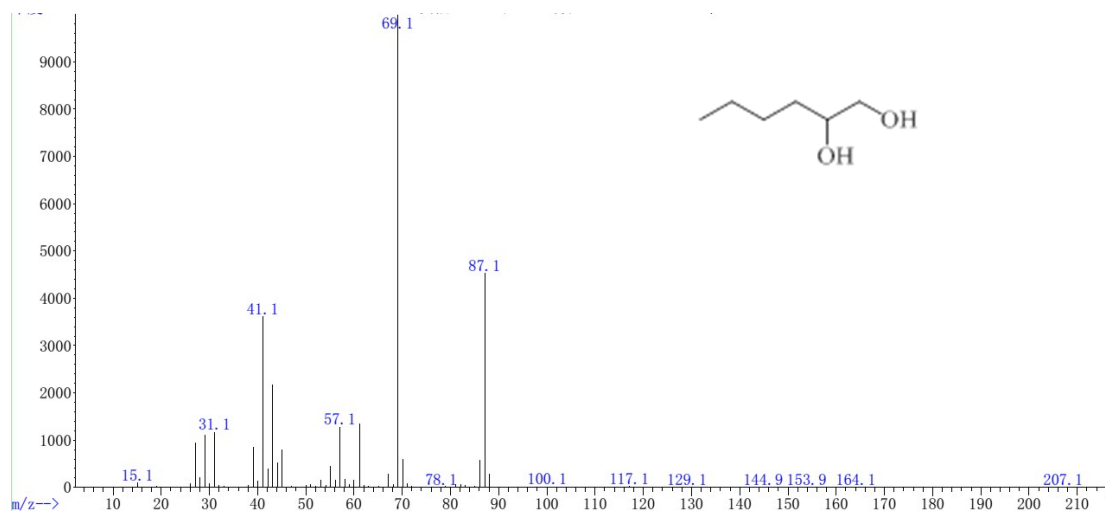


Fig. S7

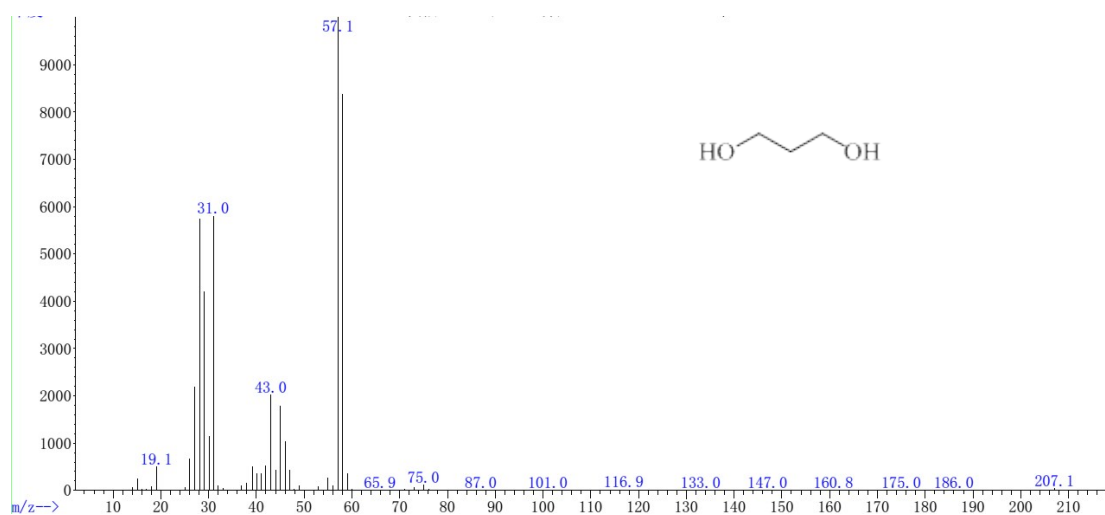


Fig. S8

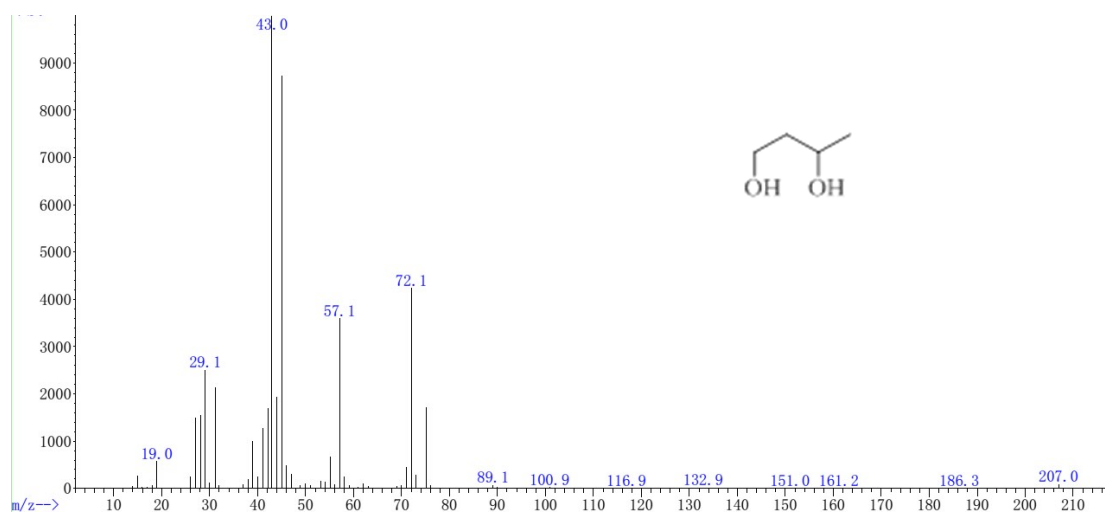


Fig. S9

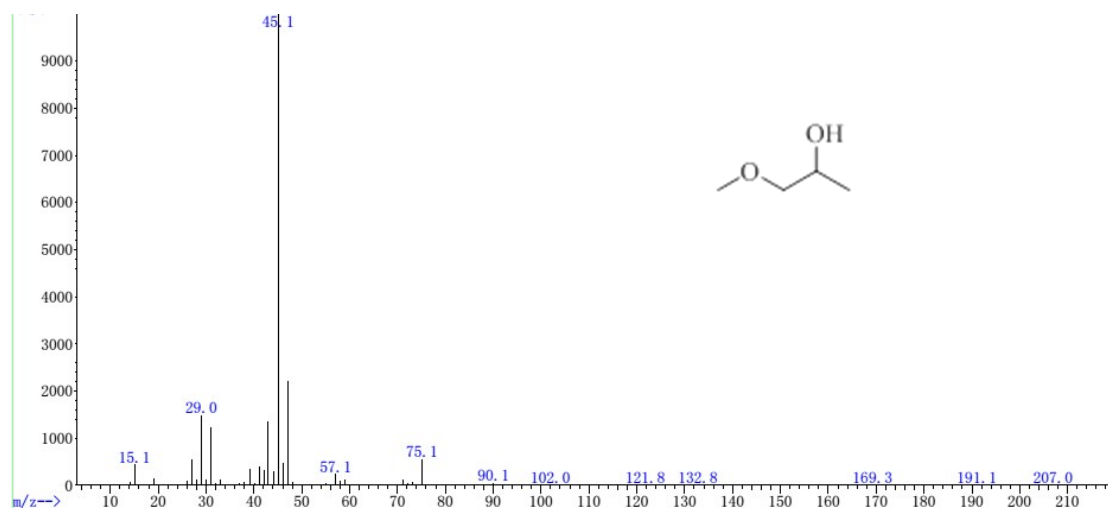


Fig. S10

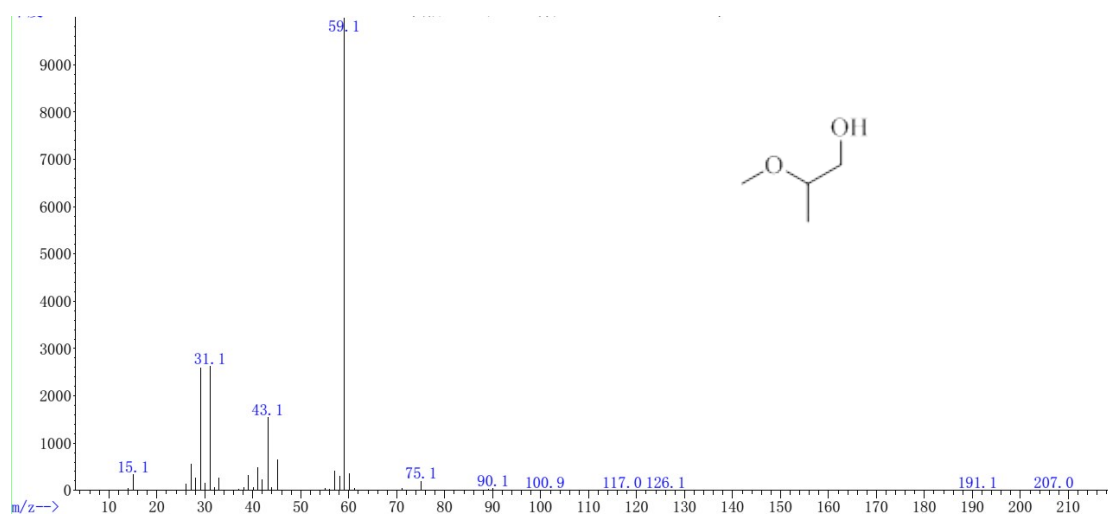


Fig. S11

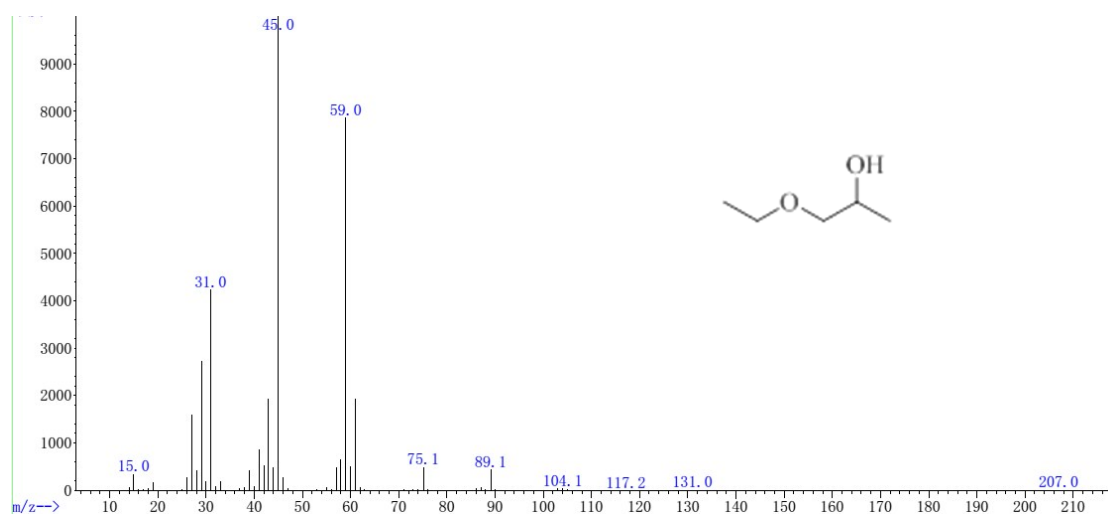


Fig. S12

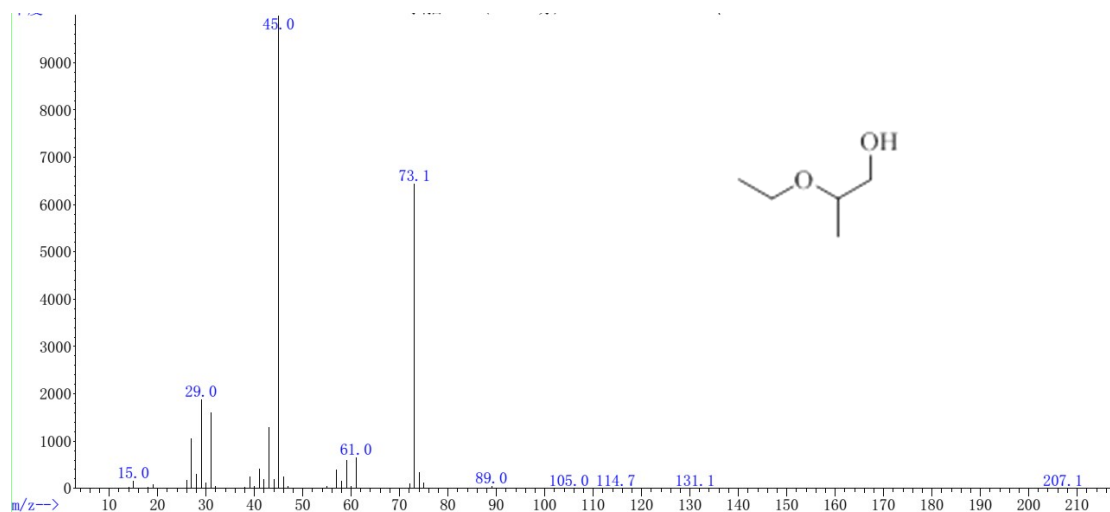


Fig. S13

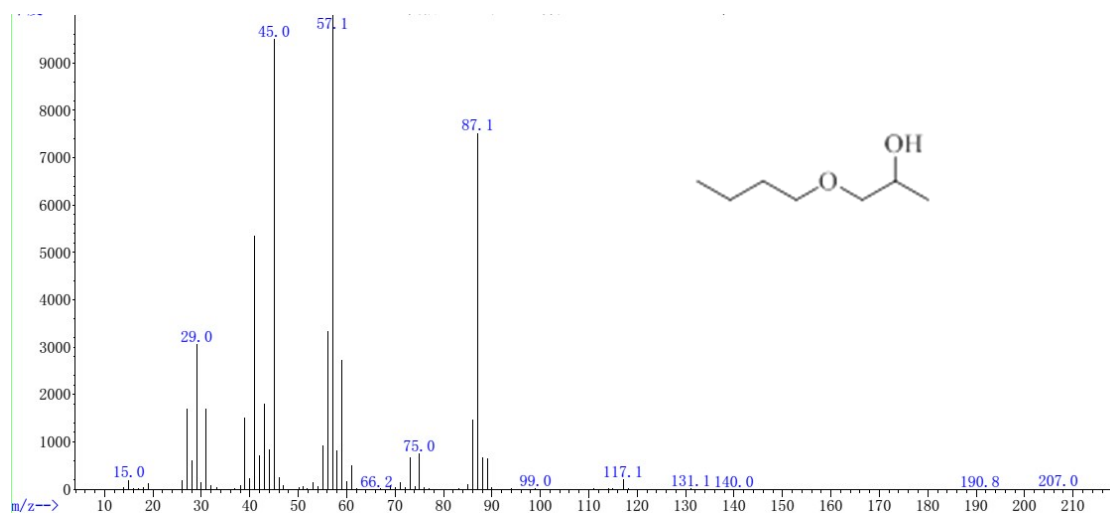


Fig. S14

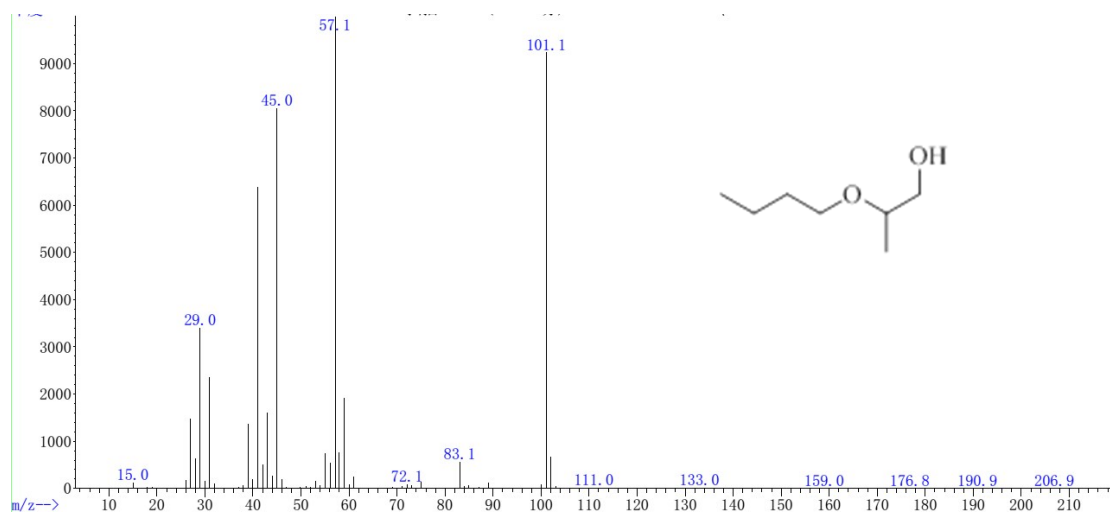


Fig. S15

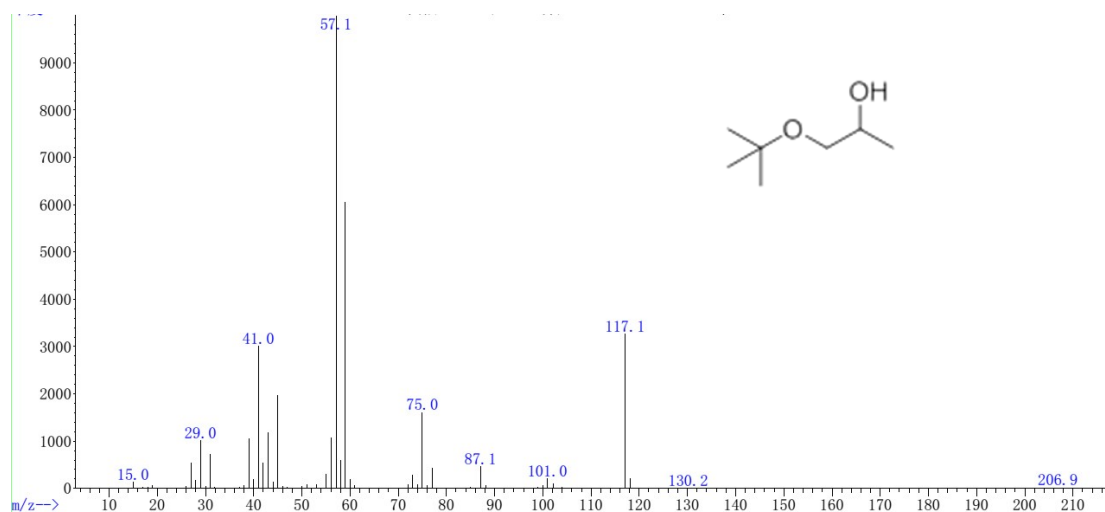


Fig. S16

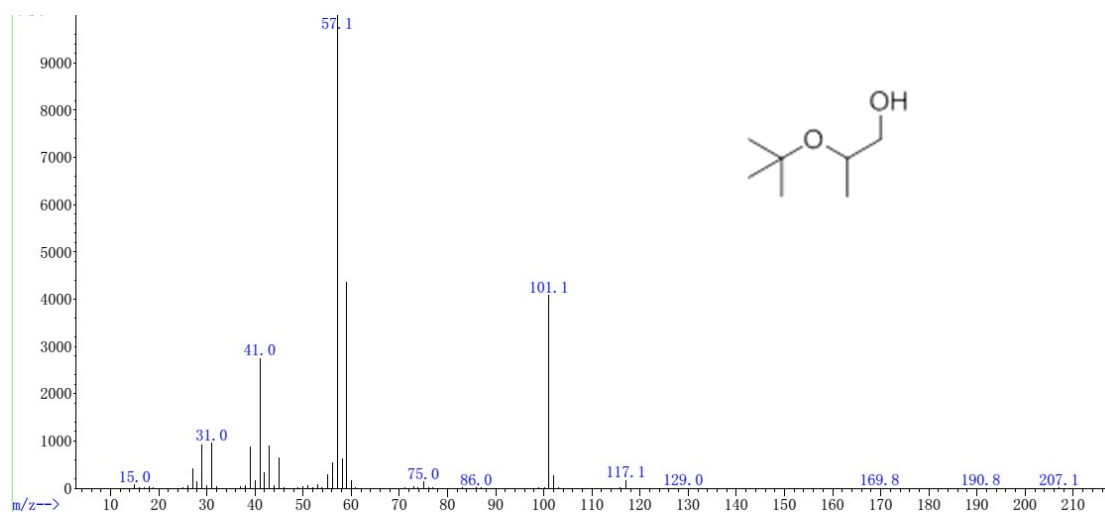
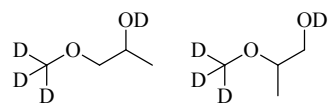


Fig. S17

In the hydrolysis and alcoholysis catalysis, the products were separated from the reaction system and characterized with  $^1\text{H}$  NMR and  $^{13}\text{C}$  NMR. The spectrum of some products are showed as follows (Fig. S18- Fig. S22):



$^1\text{H}$  NMR (400 MHz,  $\text{CD}_3\text{OD}$ ) 3.87 (d,  $J=5.2$  Hz, 1H), 3.84-3.23 (m, 24H), 1.11 (t,  $J=6.4$  Hz, 13H).

$^{13}\text{C}$  NMR (101 MHz,  $\text{CD}_3\text{OD}$ )  $\delta=77.91, 77.62, 65.80, 64.87, 57.94, 55.45, 18.38, 14.79$ .

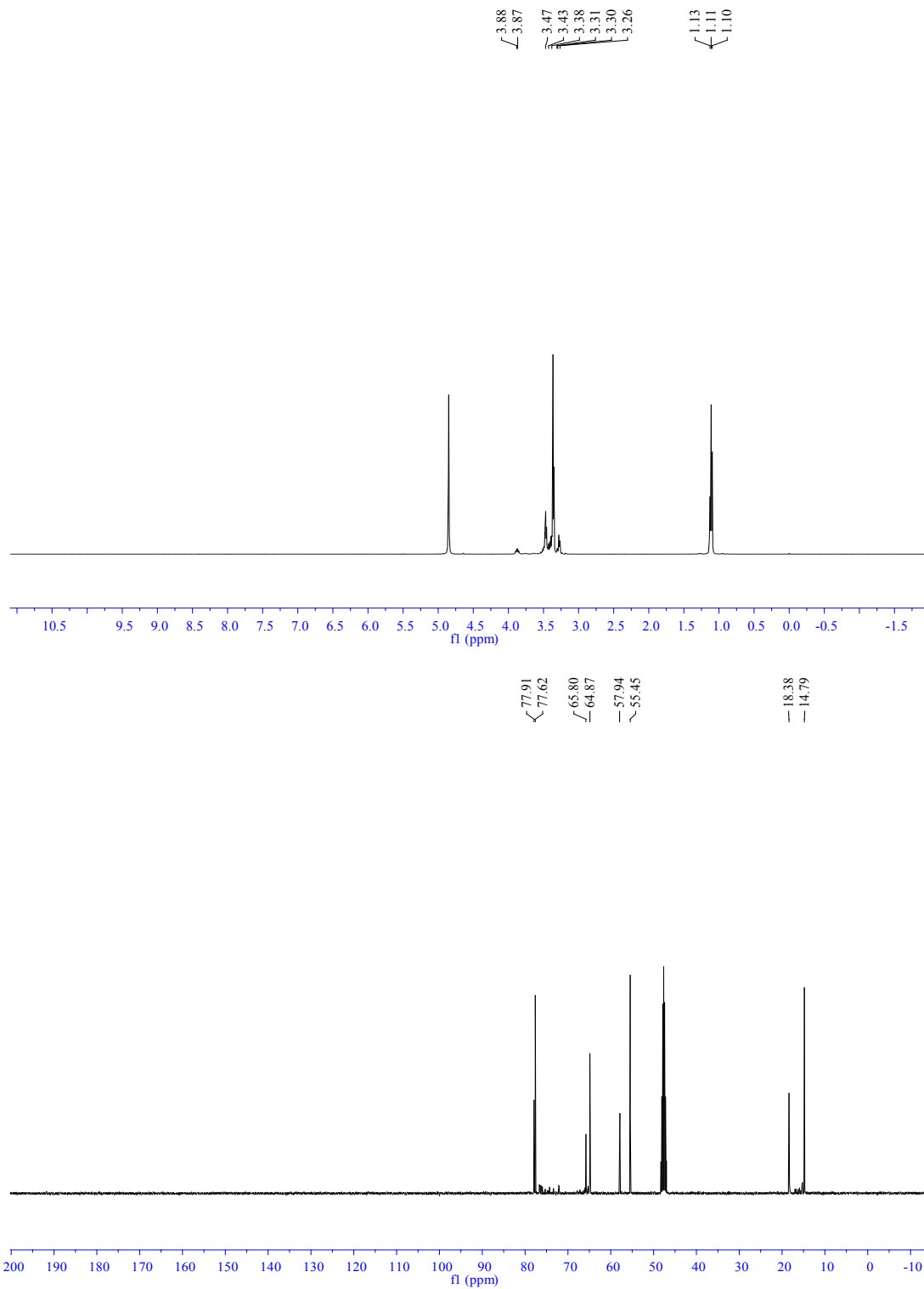
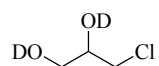


Fig. S18



$^1\text{H}$  NMR (400 MHz,  $\text{D}_2\text{O}$ )  $\delta$ =3.92-3.84 (m, 1H), 3.69-3.59 (m, 2H), 3.56 (ddd,  $J$ =11.7, 6.0, 2.8 Hz, 2H).

$^{13}\text{C}$  NMR (101 MHz,  $\text{D}_2\text{O}$ )  $\delta$ =71.14, 62.54, 45.92.

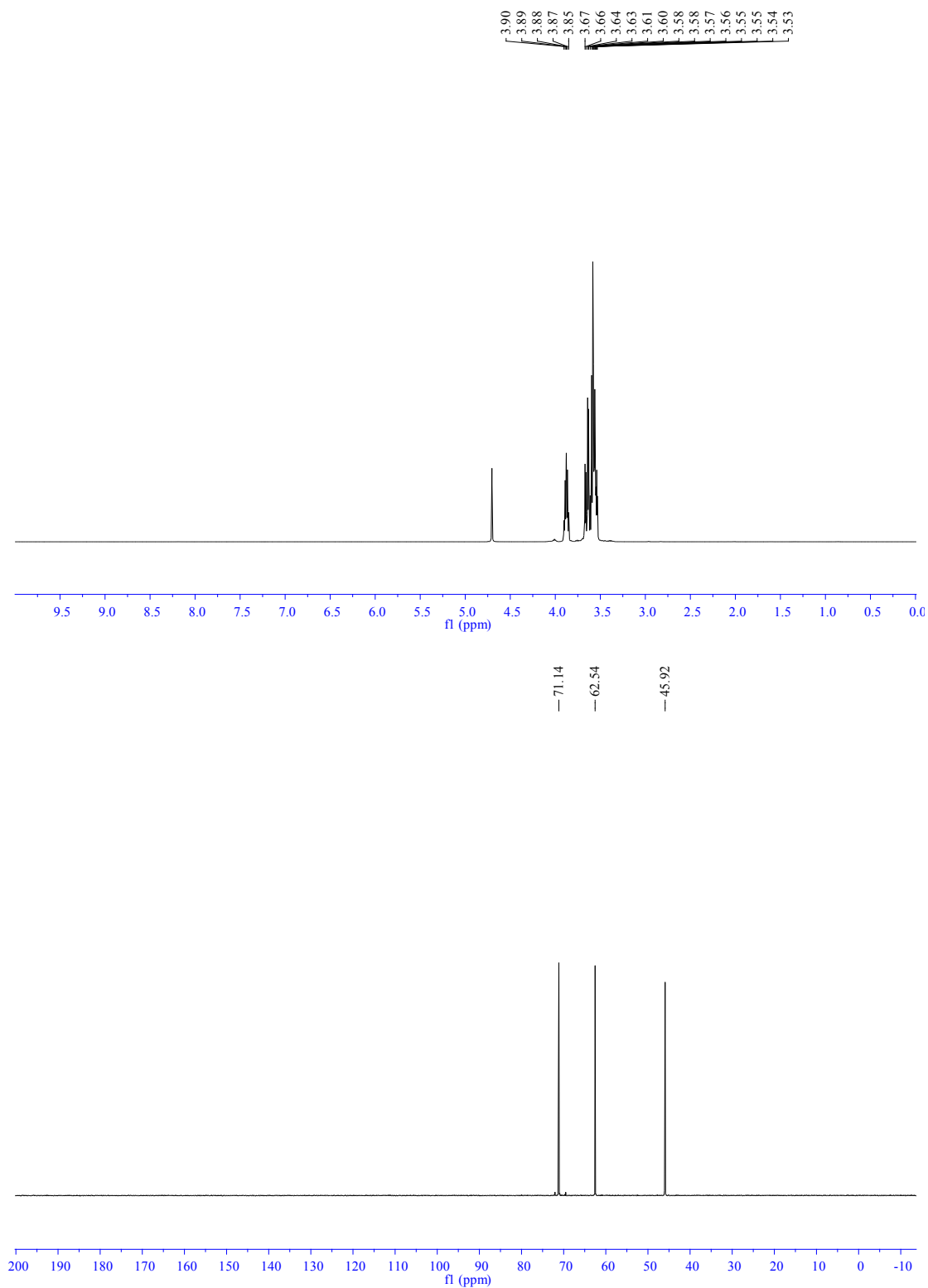
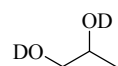


Fig. S19



$^1\text{H}$  NMR (400 MHz,  $\text{D}_2\text{O}$ )  $\delta$ =3.78-3.68 (m, 1H), 3.35 (ddd,  $J$ =18.2, 11.5, 5.5 Hz, 2H), 1.01 (d,  $J$ =6.5 Hz, 3H).

$^{13}\text{C}$  NMR (101 MHz,  $\text{D}_2\text{O}$ )  $\delta$ =67.85, 66.58, 18.09.

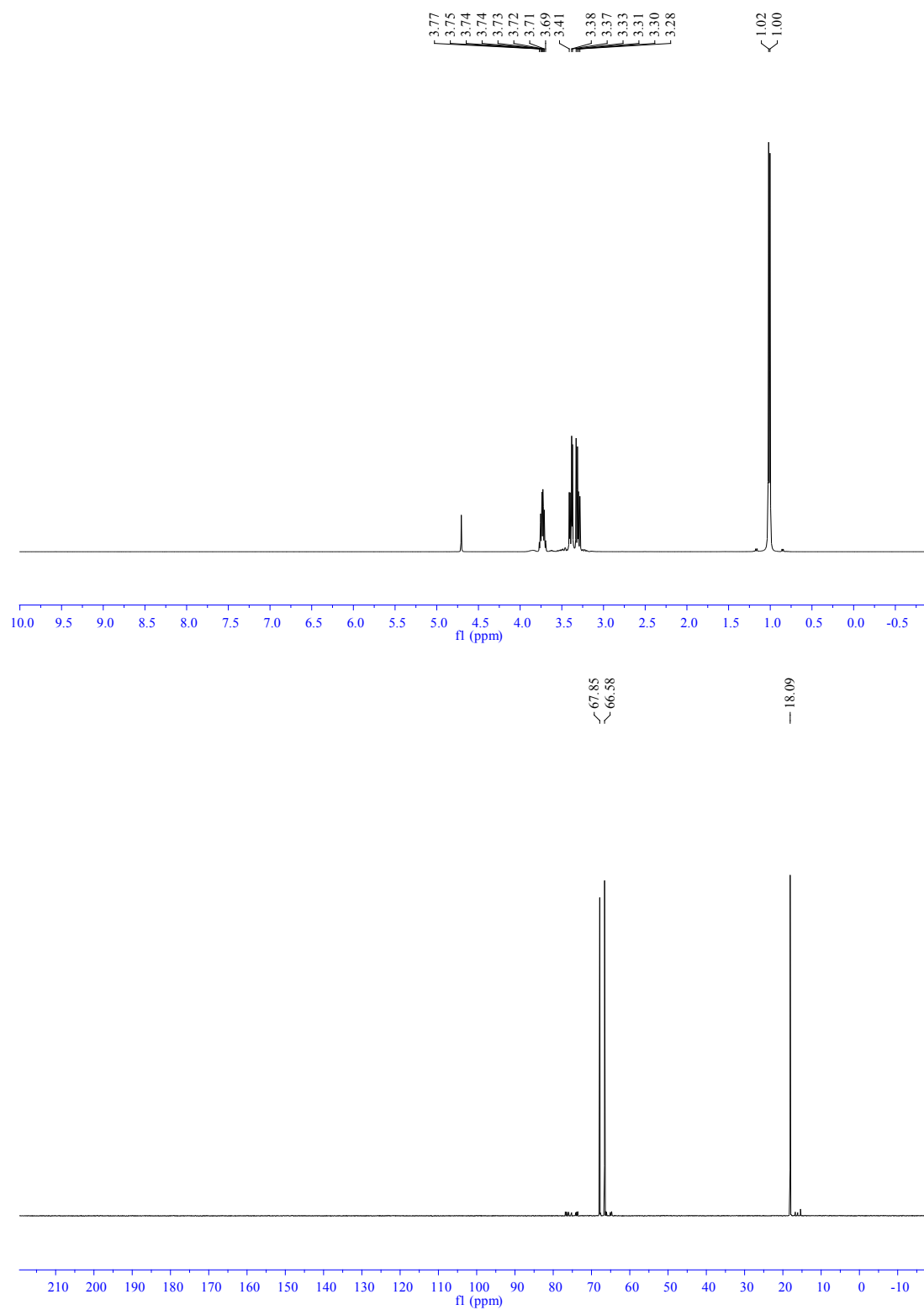
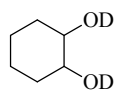


Fig. S20



$^1\text{H}$  NMR (400 MHz,  $\text{D}_2\text{O}$ )  $\delta$ =3.48-3.17 (m, 2H), 1.95-1.76 (m, 2H), 1.66-1.48 (m, 2H), 1.16 (d,  $J$ =4.5 Hz, 4H).

$^{13}\text{C}$  NMR (101 MHz,  $\text{D}_2\text{O}$ )  $\delta$ =74.81, 32.55, 23.80.

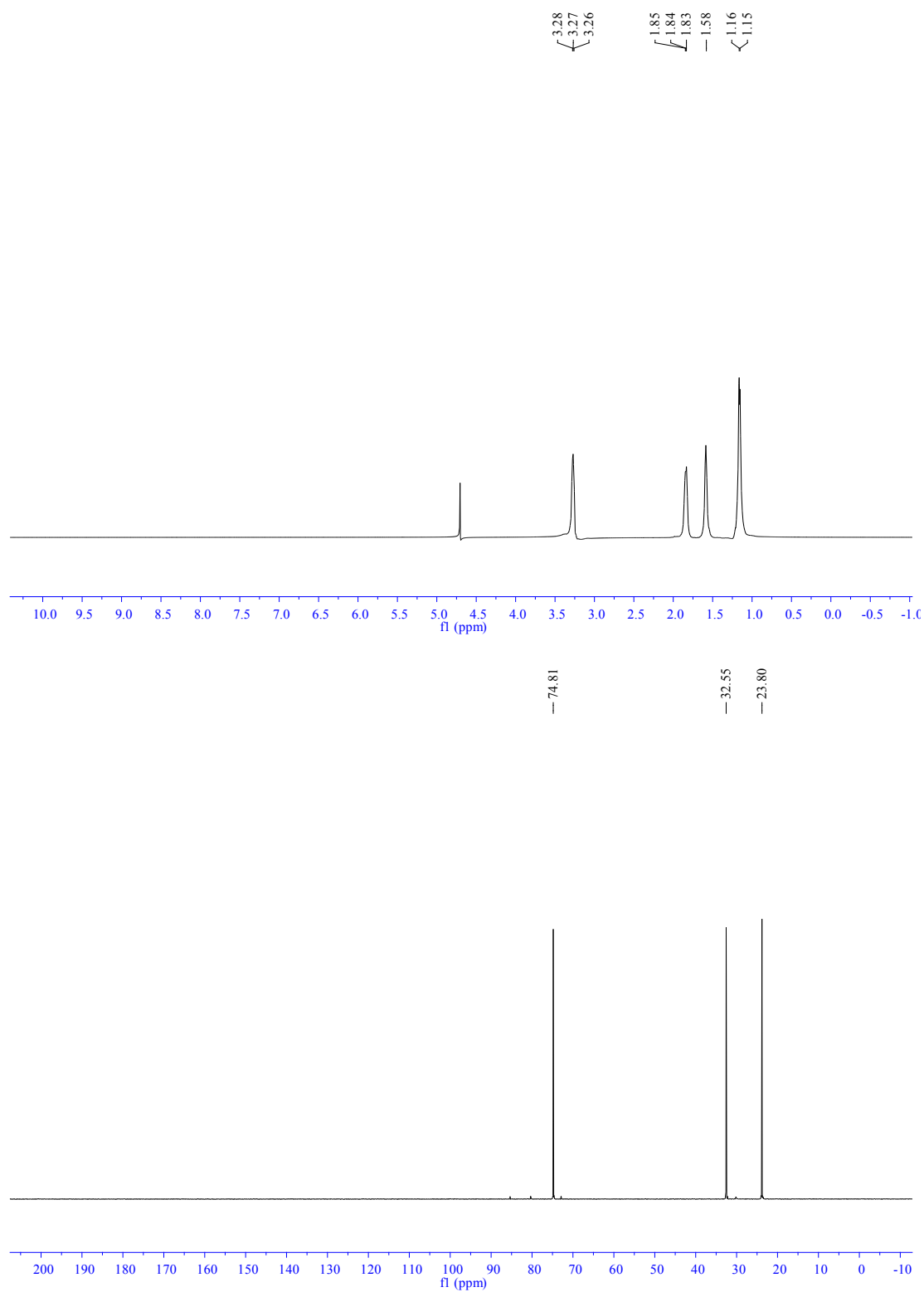
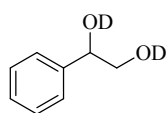


Fig. S21



$^1\text{H}$  NMR (400 MHz,  $\text{D}_2\text{O}$ )  $\delta$ =7.36-7.21 (m, 5H), 4.67 (t,  $J$ =6.0, 1H), 3.60 (d,  $J$ =6.0 Hz, 2H).

$^{13}\text{C}$  NMR (101 MHz,  $\text{D}_2\text{O}$ )  $\delta$ =140.54, 128.65, 128.09, 126.39, 74.06, 66.31.

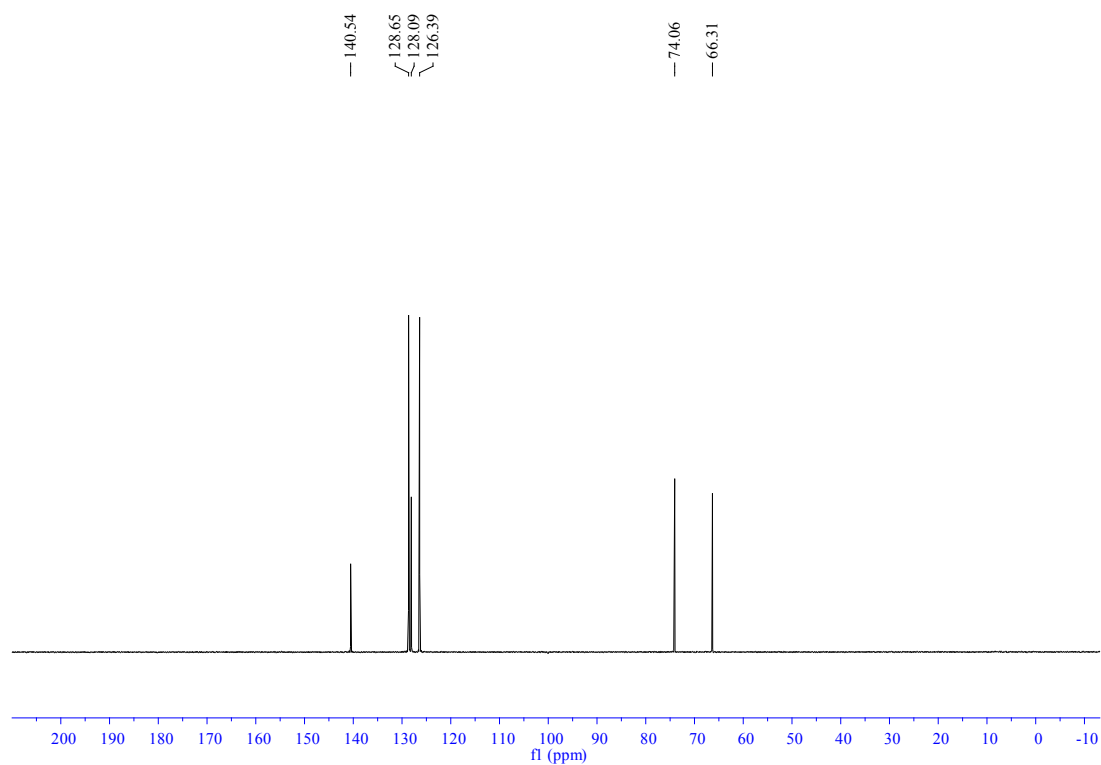
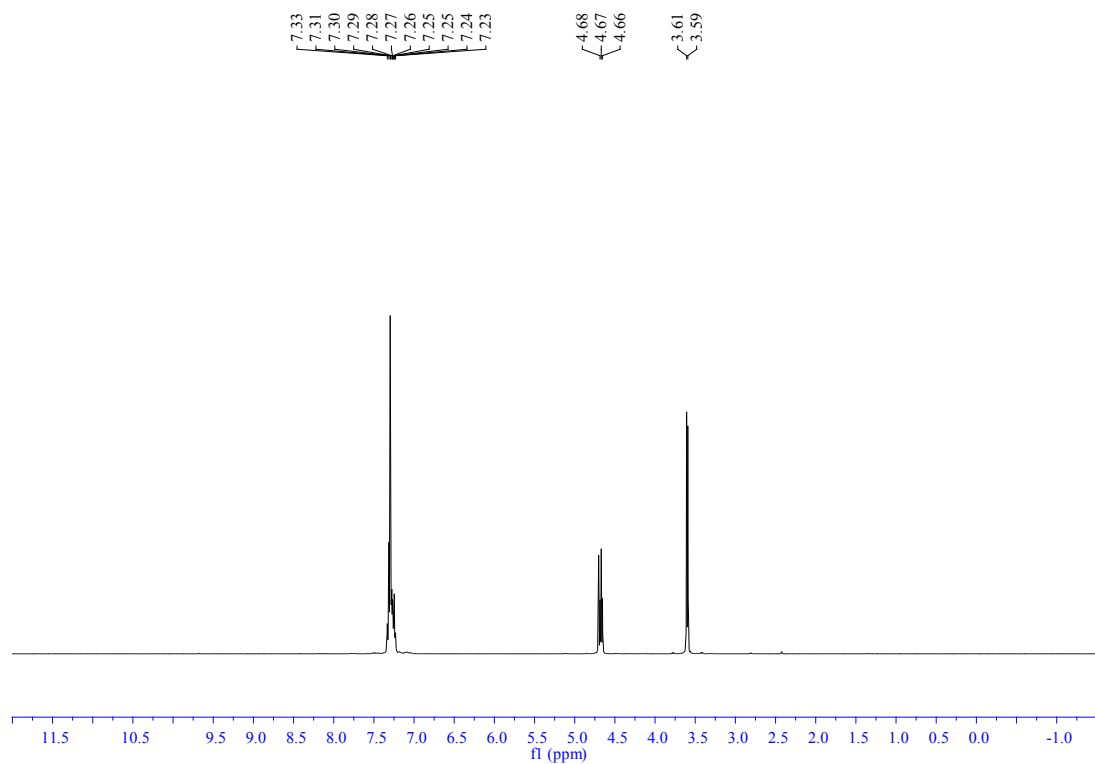


Fig. S22